The Electro-Oxidation of Ethanol in Alkaline Medium at Different Catalyst Metals

Domnik Bayer, Carsten Cremers, Helmut Baltruschat and Jens Tübke

ECS Trans. 2011, Volume 41, Issue 1, Pages 1669-1680.
doi: 10.1149/1.3635698

ECS Transactions, 41 (1) 1669-1680 (2011)
10.1149/1.3635698 ©The Electrochemical Society

The Electro-Oxidation of Ethanol in Alkaline Medium at Different Catalyst Metals

D. Bayer[1], C. Cremers[1], H. Baltruschat[2] and J. Tübke[1]

[1] Fraunhofer-Institute for Chemical Technology ICT, Applied Electrochemistry
76327 Pfinztal, Germany
[2] Institute for Physical and Theoretical Chemistry, University of Bonn
53117 Bonn, Germany

In this contribution, the electro-oxidation of ethanol in alkaline medium is studied with differential electrochemical mass spectrometry (DEMS). Starting from platinum as model catalyst, the influence of the catalyst on the ethanol oxidation reaction is investigated with other metals, i.e. palladium, gold and nickel. It was found that the reaction products and their current efficiencies depend strongly on the catalyst used. At platinum the reaction to acetate is the major current producing path while the current efficiency for carbon dioxide is low. At higher ethanol concentrations ethyl acetate is formed. During the ethanol oxidation at palladium the current efficiency for acetate is even higher and only traces of carbon dioxide are formed. However, an ethyl acetate formation was not observed. Gold shows a significant activity for the ethanol oxidation with ethyl acetate being the only detected product. The activity of nickel towards the ethanol oxidation in alkaline medium is negligible.

Introduction

Alkaline direct alcohol fuel cells (ADAFC) can be an interesting alternative for the future power supply of portable devices with low energy demands and long projected operating times (1). There are basically two advantages for choosing an ADAFC compared to other fuel cell types: First, direct alcohol fuel cells (DAFC) guarantee an intrinsically long operating period due to the comparatively high energy density of the fuel. Methanol, which is already a common fuel for acidic DAFC, has an energy density of 6.1 kWh kg^{-1} while the energy density of ethanol is even higher (7.4 kWh kg^{-1}). Moreover, methanol is classified as a toxic chemical while ethanol is commercially available without restrictions when it is denatured (2). A second reason for the prospective high potential of ADAFC is the alkaline medium itself. It has been shown that the kinetics of the alcohol oxidation in alkaline medium is enhanced (3, 4). This is especially true for ethanol (5). This fact is mostly ascribed to the higher concentration of hydroxyl species in alkaline medium which play a key role in the removal of poisoning species from the catalyst surface (6, 7). Furthermore, the enhanced reaction kinetics and the lower corrosivity of the medium enable the use of non-noble metal catalysts. This in combination with the application of comparatively cheaper anion exchange membranes renders ADAFC a potential low cost alternative to the already established acidic direct methanol fuel cells (1), for example.

However, fast kinetics and especially a high energy density of the fuel can only be considered an advantage when the complete conversion of the fuel to carbon dioxide is achieved. This is especially challenging for longer chained alcohols as it involves a scission of the carbon-carbon bond. As the reaction mechanisms of higher alcohols in alkaline medium are still not completely elucidated, a number of recent publications have appeared in this field (8, 9). Furthermore, it has been shown that complete conversion of higher alcohols at platinum is not obtained (10). This underlines the need to find more selective catalysts for the complete oxidation of higher alcohols in order to retain or even boost the attractiveness of ADAFC.

In this respect, several metals could be suitable candidates to replace the costly platinum. Above all, apart from platinum based catalysts, palladium seems to be promising as it is said to have a higher activity for the ethanol oxidation than pure platinum (11, 12). Also gold shows a certain activity for the alcohol oxidation in alkaline medium (13, 14). Some authors report on the catalytic activity of nickel for the oxidation of organic molecules (15), and it seems that nickel has at least a positive co-catalytic effect on the alcohol oxidation (1).

This article reports on the results of an ongoing study on the influence of the catalyst metal on the electro-oxidation of ethanol. Exceeding purely electrochemical experiments, differential electrochemical mass spectrometry (DEMS) is employed to obtain qualitative and quantitative information on formed reaction products. Based on earlier publications the electro-oxidation of ethanol at platinum is studied as a reference. As a starting point the alternative metals palladium, gold and nickel are investigated.

Experimental

In this study, the alkaline solutions were prepared from ultrapure water (0.055 μS cm^{-1}) and 0.1 M potassium hydroxide (Sigma Aldrich, *Trace*SELECT®, 99.995%). Ethanol was purchased from Merck (p.a., 99.9%) and used as received. For catalysts with higher activity, an ethanol concentration of 0.01 M in 0.1 M potassium hydroxide was used while catalysts with a lower activity were studied in 0.1 M ethanol / 0.1 M potassium hydroxide solution. All potentials are referenced to the reversible hydrogen electrode (RHE). Unless otherwise stated, reported current densities refer to the surface area determined in carbon monoxide stripping experiments.

DEMS Setup and Calibration

The principles of flow cells used in DEMS are explicitly described in (16). However, the cell used here is modified in order to suit the special requirements of product detection in alkaline medium. With regard to DEMS, one disadvantage of the alkaline medium is the conversion of carbon dioxide into carbonate. Carbonate is not volatile and thus undetectable with DEMS. However, in (17) and (9) it was shown that carbon dioxide can be detected if formed at sputtered electrodes. The reason is the slow reaction to carbonate from the preliminarily formed carbon dioxide.

The body of the flow cell used in this study was made from PCTFE. In analogy to the dual thin layer flow-through cell described in (18), the thin layer flow cell used here

consisted of two compartments. However, the difference is that the detection compartment is simultaneously used as reaction compartment by employing a membrane with a sputter deposited catalyst metal as working electrode and interface between electrolyte and vacuum. The advantage of this configuration is the immediate transfer of product species, e.g. carbon dioxide, into the vacuum system right after their formation without having the time to react with the surrounding electrolyte. The second compartment is used as counter electrode compartment and electrolyte outlet. This setup combines the short response times of a membrane electrode inlet and the defined mass transport of the dual thin layer flow-through cell. By replacing one catalyst coated membrane by another, the catalyst can be exchanged without altering the cell geometry. The flow cell used in this work is shown in figure 1.

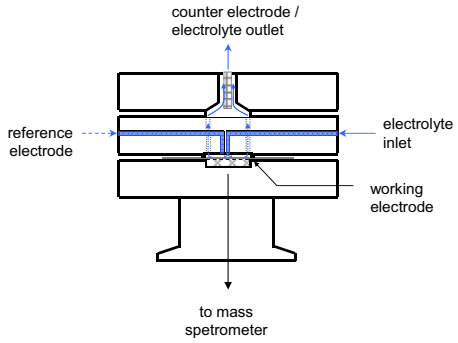

Figure 1. Schematic representation of the thin layer flow cell for the detection of volatile reaction products in alkaline environment.

With a diameter of 1 cm and a cell height of 0.2 mm, the volume of the working electrode compartment excluding connecting capillaries is approximately 16 µl. The response time determined according to the procedure given in (19) is only 272 ms.

Calibration of the mass spectrometer for carbon dioxide can be obtained by carbon monoxide stripping experiments or by potentiostatic oxidation carbon monoxide saturated base electrolyte. The procedure for the carbon dioxide calibration in alkaline medium is already described and evaluated in (9). For a better understanding it will be repeated exemplarily.

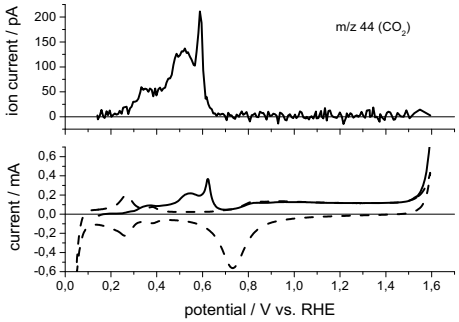

Figure 2. Background corrected mass spectrometric ion current for m/z 44 (above) and Faradaic current (below) for the oxidation of adsorbed carbon monoxide at a platinum electrode in 0.1 M KOH. Stripping voltammogram (line) and background voltammogram (dashed).

Carbon monoxide is adsorbed on the working electrode from carbon monoxide saturated electrolyte. Afterwards the electrolyte is replaced by base electrolyte without carbon monoxide and an anodic stripping cycle is started. In this stripping cycle, carbon monoxide is exclusively oxidized to carbon dioxide. As shown in figure 2, the Faradaic current and the respective mass spectrometric ion current coincide.

In order to obtain a calibration, the Faradaic charge has to be correlated with the amount of formed carbon dioxide which is represented by the mass spectrometric charge taking into account the number of electrons transferred per formula unit. The resulting calibration constant for carbon dioxide can be obtained as described in equation [1].

$$K^*_{CO2} = 2 * Q_{MS,m/z\ 44} / Q_F \qquad [1]$$

In equation [1], K^*_{CO2} stands for the calibration constant, $Q_{MS,m/z\ 44}$ represents the integrated background corrected ion current of the mass to charge ratio 44, Q_F denotes the Faradic charge and 2 is the number of transferred electrons per molecule of carbon dioxide.

Assuming that during the oxidation of ethanol only the three products acetaldehyde, acetic acid or in alkaline medium rather acetate and carbon dioxide are formed, one has to calibrate and measure at least two of these products in order to be able to calculate the whole product spectrum. As acetate is highly soluble in alkaline electrolyte, it is undetectable with DEMS. Acetaldehyde on the other hand is volatile enough to be detected. However, as there is no electrochemical reaction at platinum forming acetaldehyde exclusively, its calibration is more complex. Therefore, an indirect calibration with the analog reaction from 2-propanol to acetone is chosen (20). In alkaline medium acetone is the single oxidation product of 2-propanol. Here, it is assumed that due to similar volatility from the aqueous solution and similar diffusion coefficients, the calibration constants are very similar. Figure 3 shows the Faradaic current and the respective mass spectrometric ion current for the 2-propanol oxidation at platinum.

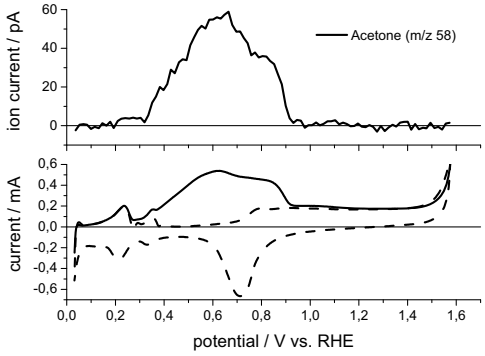

Figure 3. Background corrected ion current for m/z 58 (above) and Faradaic current (below) for the bulk oxidation of 0.01 M 2-propanol / 0.1 M KOH at platinum. Anodic branch of the voltammogram in 2-propanol solution (line) and background voltammogram in base electrolyte (dashed).

According to equation [2] following the procedure described above for carbon dioxide, a calibration constant for acetone can be obtained.

$$K^*_{acetone} = 2 * Q_{MS,m/z\ 58} / Q_F \quad [2]$$

In order to correlate the ion currents for acetone and acetaldehyde, known quantities of both substances were mass spectrometrically detected via a capillary inlet system. This yields the correlation factor F according to equation [3].

$$F_{a/b} = (I_{MS,a} * M_a * m_b) / (I_{MS,b} * M_b * m_a) \quad [3]$$

In equation [3], the index a stands for acetaldehyde, and the index b stands for acetone. I_{MS} are the ion currents of the chosen mass fragments for the respective substances while M and m represent their molecular weight and their mass quantity. For acetaldehyde the mass to charge ratio 15 was used for calibration, while acetone was detected on m/z 58. Thus, as shown in equation [4], the calibration constant for acetaldehyde can be obtained by combining the calibration constant for acetone with the correlation factor F.

$$K^*_{acetaldehyde} = F_{a/b} * K^*_{acetone} \quad [4]$$

As carbon dioxide and acetaldehyde can now be quantified, the remaining reaction product acetate can be calculated.

Results

In the following, different catalyst metals will be investigated concerning their activity towards the ethanol oxidation. Where applicable, reaction products will be identified and quantified according to the methodology described above. As a reference, the oxidation of ethanol at platinum is investigated including results from previous studies (9).

Platinum

From our previous studies (9) and other literature (8) it is known that also in alkaline solution ethanol adsorbs dissociatively at a clean platinum surface, thereby forming two distinct C_1 adsorbate species of which one can be identified as adsorbed carbon monoxide delivering a straight number of two electrons transferred per molecule of carbon dioxide formed. The second one is probably an alkyl species as it can be reduced to methane or oxidized to carbon dioxide at potentials above 0.9 V, thereby transferring a number of electrons higher than two. This is similar to what has been found for acidic solution (21, 22). As the adsorbates from methanol and carbon monoxide cannot be reduced to methane it is obvious that this adsorbate stems from the methyl group of the ethanol molecule.

In contrast to the desorption of ethanol adsorbates, the carbon dioxide formation during ethanol bulk oxidation is rather slow. Here, mainly incomplete oxidation products are formed. This is especially true for potentiostatic experiments. The contribution of the formation of each product to the total current can be assessed by calculating the current efficiency CE for each product according to equation [5].

$$CE = n * I_{MS} / (I_F * K^*) \quad [5]$$

In this general equation n represents the number of electrons transferred during bulk oxidation of ethanol to the respective product, I_{MS} and I_F are the specific mass spectrometric ion current and the Faradaic current and K^* stands for the product-specific calibration constant. The current efficiencies for carbon dioxide and acetaldehyde can be directly calculated as their calibration constants were obtained in the calibration experiments described above. Knowing the current efficiencies of the two other oxidation products, the current efficiency of the third oxidation product acetate can be calculated. Figure 4 shows exemplarily selected ion currents and the Faradaic oxidation current during ethanol oxidation at platinum.

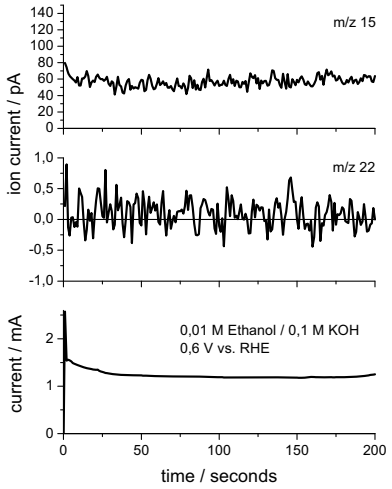

Figure 4. Background corrected ion currents m/z 15 and m/z 22 (above) and Faradaic current (below) for the potentiostatic oxidation of 0.01 M ethanol / 0.1 M KOH at platinum at 0.6 V vs. RHE.

As it can be seen from figure 4, the signal for carbon dioxide (m/z 22, CO^{++} fragment) has a low signal to noise ratio. So in order to get more reliable data, the arithmetic mean of the last 20 seconds of each signal was taken to calculate the current efficiencies.

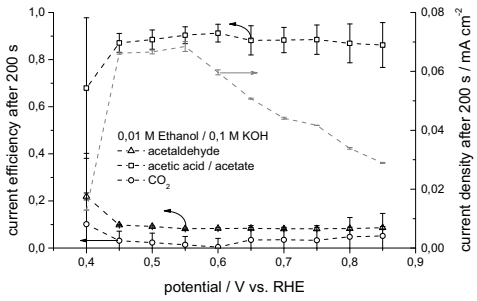

Figure 5. Current efficiencies for acetaldehyde (triangles), acetate (squares) and carbon dioxide (circles) as well as steady state current density (grey) for the potentiostatic oxidation of 0.01 M ethanol / 0.1 M KOH at platinum for various potentials.

Figure 5 shows that the main current producing path during oxidation of ethanol is the reaction to acetate. Except at low potentials, the reaction to acetaldehyde has a current efficiency of around 10%. Carbon dioxide is a minor product of the ethanol oxidation; its current efficiency is predominantly below 5% unless at the lowest investigated potential. This means that the oxidation of ethanol proceeds under the given circumstances essentially through incomplete oxidation. Looking at the average electron yield, depending on the potential, 3.9 to 4.1 electrons out of 12 possible electrons per formula unit for the total oxidation to carbon dioxide are obtained.

For ethanol concentrations higher than 0.05 M, the formation of ethyl acetate as reaction product is observed.

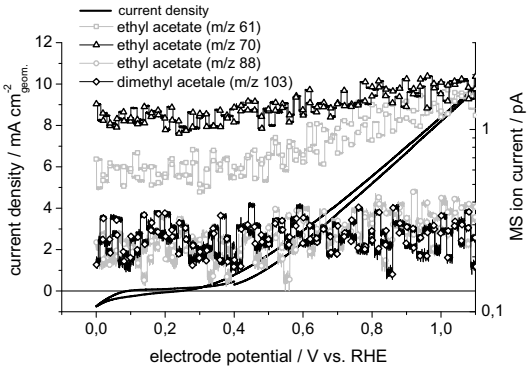

Figure 6. Background corrected ion currents for m/z 61, 70, 88 (ethyl acetate) and m/z 103 (dimethyl acetale) as well as current density for the potentiodynamic oxidation of 0.1 M ethanol / 0.1 M KOH at platinum.

As the ethyl acetate formation in figure 6 is potential induced and does not take place when an ethanol and acetate containing solution is flushed through the flow cell at open circuit potential, this is not a secondary reaction of the acetate formation taking place in the bulk electrolyte but a reaction taking place at the electrode surface, similar to what has been found for the formation of methyl formate during methanol oxidation (23).

Palladium

Compared to platinum, palladium is an alternative catalyst metal also known from the chemical industry. However, depending on the market, the price of palladium is only about one third of the price of platinum.

As shown in figure 7, the oxidation of adsorbed carbon monoxide at palladium begins at around 0.35 V, and thus at a slightly higher potential than the carbon monoxide oxidation at platinum (9). Following a sharp peak at around 0.73 V, only traces of carbon monoxide are oxidized until a potential of 1.1 V is reached. After having reached the anodic vertex potential, the carbon monoxide is removed quantitatively from the electrode surface and the background voltammogram is obtained.

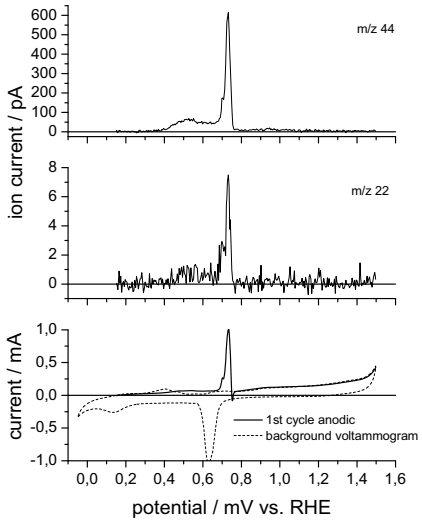

Figure 7. Background corrected ion currents m/z 44 and m/z 22 as well as Faradaic current of the anodic stripping voltammogram (line) and background voltammogram (dashed) for the oxidation of pre-adsorbed carbon monoxide at palladium in 0.1 M KOH.

As shown in figure 8, the oxidation of the ethanol adsorbates begins at around 0.4 V to 0.5 V and goes on after a peak at approximately 0.72 V until a potential of 1.2 V is reached.

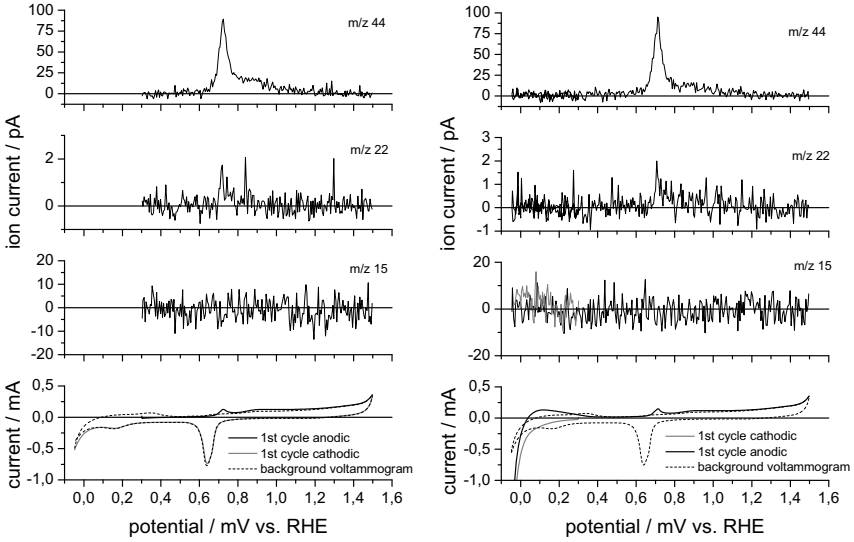

Figure 8. Background corrected ion currents for m/z 44, 22 and 15 (above) and Faraday currents for the anodic (black line) and cathodic branch (grey line) of the first potential cycle including background voltammogram (dashed). Stripping voltammogram started from the adsorption potential of 0.3 V in anodic (left) and cathodic direction (right). Palladium electrode saturated from 0.01 M ethanol / 0.1 M KOH for 300 s.

An analysis of the integrated ion current for carbon dioxide (m/z 44 or m/z 22) in comparison with the results from the carbon monoxide stripping experiment in figure 7 yields a relative surface coverage of carbon monoxide from the ethanol adsorption of θ_{CO} = 0.27. Under similar conditions, a value of θ_{CO} = 0.45 is obtained for ethanol at platinum. Furthermore, at palladium, the analysis of the number of electrons transferred per molecule of carbon dioxide formed yields 2.1 electrons (figure 8, left hand side) or 1.9 electrons (figure 8, right hand side) over the whole potential range indicating that no other adsorbate than adsorbed carbon monoxide is oxidized to carbon dioxide and probably not present on the electrode surface. Correspondingly, no significant methane formation in cathodically started stripping voltammograms is detected (cf. m/z 15, figure 8 right).

For palladium, the calibration for acetaldehyde can be obtained in a similar manner as for ethanol as here the exclusive product of the 2-propanol oxidation is again acetone. Figure 9 shows the current efficiencies for the potentiostatic bulk oxidation of ethanol at palladium obtained from experiments consistent with the ones conducted at platinum.

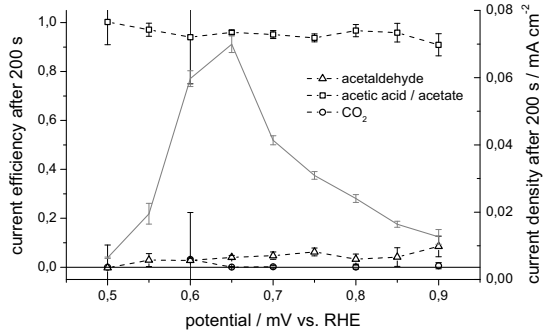

Figure 9. Current efficiencies for acetaldehyde (triangles), acetate (squares) and carbon dioxide (circles) as well as steady state current density (grey) for the potentiostatic oxidation of 0.01 M ethanol / 0.1 M KOH at palladium for various potentials.

Compared to platinum, the current efficiencies for acetate at palladium are even higher (above 90%). Furthermore, carbon dioxide formation is negligible if it can be detected at all. Also the current efficiency for acetaldehyde is below 10%, and thus lower than for the ethanol oxidation at platinum. This means that at palladium acetate is formed almost selectively. Accordingly, the average electron yield is dependent on the potential between 3.9 and 4.0. Even at higher concentrations of 0.1 M ethanol, a formation of ethyl acetate was not observed at palladium.

Gold

As gold shows substantial activity for the alcohol oxidation in alkaline medium, it is subject to recent studies (13, 14).

As show in figure 10 on the left hand side, the oxidation of ethanol at gold starts at about 0.4 V corresponding to ethanol consumption as indicated by the m/z 31 signal. The oxidation current forms a pre-wave at about 0.85 V until a peak is reached at 1.1 V. Regarding the m/z 44 signal, significant formation of some product starts at around 0.9 V. However, this product seems to be neither acetaldehyde nor carbon dioxide, as no

significant activity was detected for m/z 42 (acetaldehyde) and m/z 22 (carbon dioxide). On the other hand, as shown in figure 10 on the right hand side, the formation of ethyl acetate is indicated by m/z 61 in the potential region between 0.9 and 1.25 V corresponding to the peak in the Faraday current. As the m/z 44 signal correlates with m/z 61, it is attributed to the ethyl acetate formation as well. The consumption of ethanol in the potential region between 0.4 and 0.9 V as indicated by the m/z 31 signal without detectable product formation indicates the formation of an undetectable product, i.e. acetate.

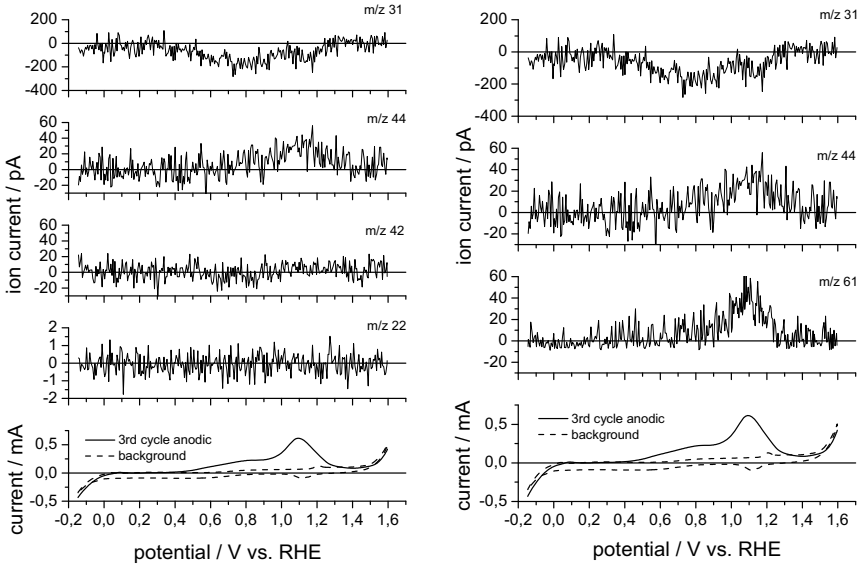

Figure 10. Background corrected ion currents for m/z 31, 44, 42 and 22 (left) as well as for m/z 31, 44 and 61 (right). In both graphs the Faradaic current (line) and the background voltammogram (dashed) for the potentiodynamic oxidation of 0.1 M ethanol / 0.1 M KOH at gold are indicated.

Thus, the assumed products of the ethanol oxidation at gold seem to be acetate and ethyl acetate.

Nickel

In the case of nickel, a slight activity for the ethanol oxidation was detected in the potential region between 0.45 and 0.95 V.

As shown in figure 11, this activity is accompanied by ethanol consumption as indicated by the m/z 31 signal. However, no detectable product is formed as exemplarily shown by the m/z 44 signal in figure 11. This leads to the assumption that the only bulk oxidation product of the ethanol oxidation at nickel is acetate.

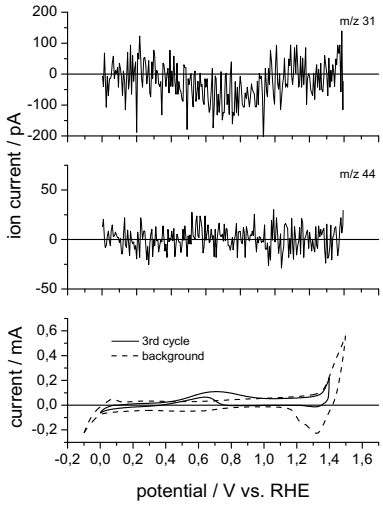

Figure 11. Background corrected ion currents for m/z 31 and m/z 44 as well as Faradaic current (line) and background current (dashed) for the potentiodynamic oxidation of 0.1 M ethanol / 0.1 M KOH at nickel.

Conclusion

In this paper, the applicability of DEMS for the product detection and determination of current efficiencies in alkaline medium has been demonstrated. The catalyst metals platinum, palladium, gold and nickel were studied with respect to their influence on the ethanol oxidation in alkaline medium.

It turned out that palladium can be an alternative catalyst metal as it showed a comparable or even a slightly higher activity for the ethanol oxidation. Regarding the ethanol adsorbates, contrarily to platinum, at palladium only adsorbed carbon monoxide seems to be present on the electrode. For palladium, the relative surface coverage with adsorbed carbon monoxide is only about 60% of that of ethanol. With respect to the current efficiencies during potentiostatic bulk oxidation at platinum (highest current efficiency for acetate, some for acetaldehyde and low current efficiency for carbon dioxide), the contribution of the acetate formation to the total oxidation current at palladium is even higher so that the one for acetaldehyde formation is lower and only traces of carbon dioxide could be detected. Another difference between platinum and palladium is the ability to form ethyl acetate at higher ethanol concentrations which was not observed at palladium.

Compared to platinum and palladium, gold showed a lower activity for the ethanol oxidation. However, as products for the oxidation of 0.1 M ethanol acetate is assumed in the lower potential region between 0.4 and 0.9 V, while the formation of ethyl acetate was detected at higher potentials.

The activity of nickel for the ethanol oxidation is very low. As ethanol consumption but no volatile product formation was detected in the potential region between 0.45 and 0.95 V, acetate is assumed to be the only oxidation product.

This preliminary analysis of four potential catalyst metals for the ethanol oxidation has shown that palladium is the only mono-metallic alternative to platinum. However, the current efficiency for the desired total oxidation product carbon dioxide is even lower at palladium than at platinum. In any case, in order to find a suitable catalyst for the ethanol oxidation in alkaline medium, more work needs to be done.

Acknowledgments

Financial support of this work by the German Federal Ministry of Defence (BMVg) is hereby gratefully acknowledged. Thanks are due to S. Ernst for helpful discussions.

References

1. E. Antolini, E. R. Gonzalez, *J. Power Sources*, **195**, 3431 (2010).
2. D. Bayer, F. Jung, B. Kintzel, M. Joos, C. Cremers, D. Martin, J. Bernard, J. Tübke, *Int. J. Electrochem.*, in press (2011).
3. K. Matsuoka, Y. Iriyama, T. Abe, M. Matsuoka, Z. Ogumi, *J. Power Sources*, **150**, 27 (2005).
4. V. Rao, Hariyanto, C. Cremers, U. Stimming, *Fuel Cells*, **7**, 417 (2007).
5. C. Cremers, D. Bayer, B. Kintzel, M. Joos, F. Jung, M. Krausa, J. Tübke, *ECS Trans.*, **16** (2), 1263 (2008).
6. J. Liu, J. Ye, C. Xu, S. P. Jiang, Y. Tong, *J. Power Sources*, **177**, 67 (2008).
7. V. Tripkovic, K. D. Popovic, J. D. Lovic, *Electrochim. Acta*, **46**, 3163 (2001).
8. S. C. S. Lai, M. T. M. Koper, *Phys. Chem. Chem. Phys.*, **11**, 10446 (2009).
9. D. Bayer, C. Cremers, H. Baltruschat, J. Tübke, *ECS Trans.*, **25** (13), 85 (2010).
10. A. Santasalo-Aarnio, Y. Kwon, E. Ahlberg, K. Kontturi, T. Kallio, M. T. M. Koper, *Electrochem. Comm.*, **13**, 466 (2011).
11. C. Xu, P. K. Shen, Y. Liu, *J. Power Sources*, **164**, 527 (2007).
12. Z. X. Liang, T. S. Zhao, J. B. Xu, L. D. Zhu, *Electrochim. Acta*, **54**, 2203 (2009).
13. J. Ye, J. Liu, C. Xu, A. P. Jiang, Y. Tong, *Electrochem. Comm.*, **9**, 2760 (2007).
14. Y. Kwon, S. C. S. Lai, P. Rodriguez, M. T. M. Koper, *J. Am. Chem. Soc.*, **133**, 6914 (2011).
15. M. Fleischmann, K. Korinek, D. Pletcher, *J. Electroanal. Chem.*, **31**, 39 (1971).
16. H. Baltruschat, *J. Am. Soc. Mass Spectrom.*, **15**, 1693 (2004).
17. U. Müller, A. Dülberg, A. Stoyanova, H. Baltruschat, *Electrochim. Acta*, **42**, 2499 (1997).
18. Z. Jusys, H. Massong, H. Baltruschat, *J. Electrochem. Soc.*, **146** (3), 1093, (1999).
19. O. Wolter, J. Heitbaum, *Ber. Bunsenges. Phys. Chem.*, **88**, 2 (1984).
20. E. Mostafa, H. Baltruschat, in preparation.
21. E. Pastor, T. Iwasita, *Electrochim. Acta*, **39**, 547 (1994).
22. U. Schmiemann, U. Müller, H. Baltruschat, *Electrochim. Acta*, **40**, 99 (1995).
23. A. A. Abd-El-Latif, H. Baltruschat, *J. Electroanal. Chem.*, (2011) accepted.